

# Robust gates for holonomic quantum computation

Giuseppe Florio,<sup>1,2</sup> Paolo Facchi,<sup>3,2</sup> Rosario Fazio,<sup>4,5</sup> Vittorio Giovannetti,<sup>4</sup> and Saverio Pascazio<sup>1,2</sup>

<sup>1</sup>*Dipartimento di Fisica, Università di Bari, I-70126 Bari, Italy*

<sup>2</sup>*INFN, Sezione di Bari, I-70126 Bari, Italy*

<sup>3</sup>*Dipartimento di Matematica, Università di Bari, I-70125 Bari, Italy*

<sup>4</sup>*NEST CNR-INFN & Scuola Normale Superiore, Piazza dei Cavalieri 7, 56126 Pisa, Italy*

<sup>5</sup>*International School for Advanced Studies (SISSA) via Beirut 2-4, I-34014 Trieste, ITALY*

(Dated: April 10, 2018)

Non Abelian geometric phases are attracting increasing interest because of possible experimental application in quantum computation. We study the effects of the environment (modeled as an ensemble of harmonic oscillators) on a holonomic transformation and write the corresponding master equation. The solution is analytically and numerically investigated and the behavior of the fidelity analyzed: fidelity revivals are observed and an optimal finite operation time is determined at which the gate is most robust against noise.

PACS numbers: 03.67.Lx, 03.65.Yz, 03.65.Vf

## I. INTRODUCTION

One of the possible alternatives to quantum information processing [1, 2], which is attracting increasing interest, is based on geometric interferometry [3, 4]. In this case, the transformations needed to implement the quantum gates are realized by making the Hamiltonian of the quantum computer dependent on a set of controlling parameters which describe suitable closed loops in an associated parameter space. In the adiabatic limit the dynamical contribution to the evolution can be factorized and the quantum gate only depends on the topological structure of the manifold. This should be contrasted with the dynamical approach to quantum computation, where the desired phase factors in the quantum gates are of dynamical origin. Geometric quantum computation has been formulated using both Abelian [5] and non-Abelian [6] holonomies. In Ref. [5] the first experimental demonstration of geometric quantum gates using nuclear magnetic resonance was presented. Since the appearance of the original proposals, several studies addressed the implementation with quantum optical [7], superconducting [8, 9] and semiconducting systems [10].

As is well known, decoherence is detrimental for quantum computation. Despite the large body of knowledge accumulated to study decoherence in open quantum systems [11], the study of geometric phases in the presence of decoherence and dissipation has started only recently, although with a few exceptions, and was certainly prompted by the interest in quantum computation. Together with many common features with the theory of open quantum systems, the analysis of decoherence in geometric interferometry rises several distinct issues that are of interest both as fundamental questions in quantum mechanics and in quantum computation. The adiabatic evolution, for example, cannot occur arbitrarily slow, as decoherence would destroy any interference. This implies that the decoherence processes should be analyzed in close connection with non-adiabatic corrections, a question which is not typically present in the non-unitary

dynamical evolution of open systems. Moreover, the period of the evolution fixes a new time scale, compared to which the different components of the bath will act differently. Finally, in the non-Abelian case the coupling to the environment may (partially) lift some degeneracy and therefore modify the holonomy itself. These are only a few examples of questions which emerge when one wants to study geometric phases in open systems.

Most of the attention on the properties of geometric phases in the presence of coupling to an external bath has focused on the Abelian [12, 13, 14, 15, 16, 17, 18, 19, 20, 21] case. There are however a few important exceptions where non-Abelian holonomies in open systems have been investigated as well [22, 23, 24, 25]. Solinas *et al.* [22] studied the influence of parametric noise on the scheme for holonomic quantum computation discussed in Ref. [10]. Parodi *et al.* [23] analyzed the effects of different spectral densities of a quantum thermal bath on the efficiency of this scheme. The quantum jump approach was applied by Fuentes-Guridi *et al.* [24] in order to understand under which circumstances holonomic quantum computation is robust against decoherence. Very recently Sarandy and Lidar [25] analyzed non-Abelian holonomies for open systems, starting from an analysis of the master equation in Lindblad form for the reduced density matrix.

The aim of this work is to study the non-adiabatic dynamics and the effects of quantum noise on the setup proposed by Duan, Cirac and Zoller [7]. We will present a class of 1-qubit holonomic quantum gates (which includes the NOT gate) that are intrinsically robust against any type of noise. The only requirement is that the noise be sufficiently small, so that a master equation can be written. The above mentioned robustness is a consequence of a peculiar property of this class of gates, namely the possibility to realize in the noiseless case a *perfect* gate transformation (i.e. with fidelity one) in a *finite* time. In particular this class exhibits fidelity revivals, that consist in an infinite number of (almost periodic) time values at which the fidelity reaches unity. The first revival

is the *optimal operational time* for a nonadiabatic gate in presence of noise, because it represents the point with the highest fidelity among all revivals, not to mention the corresponding adiabatic gate, whose fidelity is far lower. In this respect our analysis consists in a generalization to non-adiabatic holonomic quantum computation. Non-adiabatic holonomies have been discussed by Anandan [26], generalizing to the non-Abelian case the work of Aharonov and Anandan [27]. Very recently, the use of non-adiabatic phases has been discussed in the framework of geometric computation as a way to further protect the computer from decoherence [28]. In the same spirit we discuss this possibility in the non-Abelian case. We derive a master equation for the reduced density matrix of the system in the presence of a bath in the weak coupling approximation. This equation is numerically and analytically solved, displaying revivals of the fidelity and the existence of the afore-mentioned “optimal” finite operation time at which the detrimental effects of decoherence are minimized.

This paper is organized as follows. In Section II we briefly review the concept of holonomy in the absence of the environment and introduce notation. In Section III we focus our attention on the specific physical system discussed in [7] and study the role of non-adiabatic effects, which turn out to be important when discussing the realistic case of a finite time evolution in the presence of the environment, which we present in Section IV. We derive here a general master equation for time dependent Hamiltonians and, after specializing it to our case, we numerically solve it in Section V. The fidelity of the operations in the presence of noise will be discussed in detail, using the ideal case as a reference. Conclusions and further perspectives are presented in Section VI.

## II. HOLONOMIES

Let us introduce notation. Suppose that a system, governed by a non degenerate Hamiltonian that depends on time through a set of parameters, evolves adiabatically, covering a closed loop in the parameter space. Berry [29] discovered that at the end of the evolution the final state exhibits, in addition to the dynamical phase, also a geometric phase, whose structure depends only on the topological properties of the manifold on which the system has evolved.

The situation changes if the Hamiltonian possesses some degeneracies. In this case a loop in the parameter space realizes more complex geometric transformations [30]. Let us assume that the system eigenspaces (indexed by  $m$ ) are degenerate and denote by  $|m_k(t)\rangle$  their set of instantaneous eigenstates (the degeneracy index  $k$  ranging from 1 to  $N_m$ ). The instantaneous eigenstates form an orthonormal basis

$$\langle m'_{k'}(t) | m_k(t) \rangle = \delta_{mm'} \delta_{kk'}. \quad (2.1)$$

The time evolution of the quantum system is governed

by the Schrödinger equation

$$i \frac{d}{dt} |\psi(t)\rangle = H(t) |\psi(t)\rangle, \quad (2.2)$$

with  $H$  depending on  $t$  through a set of parameters  $x^\mu(t)$ . Having in mind quantum computation applications we will suppose that the family of Hamiltonians  $H(x(t))$  is iso-degenerate, i.e. that the dimensions of its eigenspaces do not depend on the parameters and that its eigenprojections  $P_m(x(t))$  have a smooth dependence on  $t$  (at least twice continuously differentiable). In particular, this implies that there is no level crossing between different eigenspaces. At each time  $t$ ,  $H(t)$  can be decomposed by using its instantaneous eigenprojections  $P_m(t) = \sum_k |m_k(t)\rangle \langle m_k(t)|$ :

$$H(t) = \sum_m \epsilon_m(t) P_m(t). \quad (2.3)$$

We define the operator  $R$ , whose action transports every eigenprojection from  $t_0$  to  $t$ ,

$$R(t, t_0) P_m(t_0) = P_m(t) R(t, t_0). \quad (2.4)$$

Its generator is hermitian ( $D(t, t_0) = D^\dagger(t, t_0)$ ) and reads

$$D(t, t_0) = -i R(t, t_0)^\dagger \frac{\partial}{\partial t} R(t, t_0). \quad (2.5)$$

In the interaction picture defined by the operator  $R$  we have

$$\tilde{H}(t, t_0) = R^\dagger(t, t_0) H(t) R(t, t_0) = \sum_m \epsilon_m(t) P_m(t_0). \quad (2.6)$$

and the evolution operator can be written as

$$U(t, t_0) = R(t, t_0) \mathbf{T} \exp \left\{ -i \int_{t_0}^t (\tilde{H}(s, t_0) + D(s, t_0)) ds \right\} \quad (2.7)$$

$\mathbf{T}$  being the chronological product. In the adiabatic limit the evolution of the state remains confined in the degenerate eigenspaces. The above evolution operator becomes block-diagonal and, in the case of cyclic evolution ( $P_m(t) = P_m(t_0)$ ), reads:

$$U(t, t_0) \sim \sum_m P_m(t_0) e^{-i \int_{t_0}^t \epsilon_m(s) ds} U_{\text{ad}}^m P_m(t_0), \quad (2.8)$$

where the geometric evolution

$$U_{\text{ad}}^m = \mathbf{P} \exp \left\{ - \oint_C A^m(x) \right\} \quad (2.9)$$

is given by a path ordered integral of the adiabatic connection  $A^m(x) = \sum_\mu A_\mu^m dx^\mu$ , with

$$A_\mu^m(x(t)) = P_m(x(t_0)) R^\dagger(x(t), x(t_0)) \times \frac{\partial}{\partial x^\mu} R(x(t), x(t_0)) P_m(x(t_0)). \quad (2.10)$$

The holonomy thus obtained is the fundamental ingredient for realizing complex geometric transformations. In the following section we will give an explicit example.

In the following we will also take into account non-adiabatic effects under the simplifying assumption that the eigenvalues  $\epsilon_m$  are time-independent and the connection (2.5) is piecewise constant. Then the operator  $D(t, t_0) = D(t_0, t_0)$  does not depend on time during the evolution  $\forall s \in [t, t_0]$ . Moreover,  $\tilde{H}(t, t_0) = H(t_0)$  in (2.6) and Eq. (2.7) reduces to the useful expression

$$U(t, t_0) = e^{i(t-t_0)D(t_0, t_0)} e^{-i(t-t_0)(H(t_0)+D(t_0, t_0))}, \quad (2.11)$$

which, in the adiabatic limit, becomes

$$U(t, t_0) \sim \sum_m P_m(t) e^{-i(t-t_0)[H(t_0)+A^m(t_0)]} P_m(t_0). \quad (2.12)$$

We will see that for a large class of gates it is possible to evaluate exactly the time evolution, including all non-adiabatic effects. The analysis of the evolution operator will enable us to find an optimal working point where the gate is robust against noise. This optimal time is related to revivals of fidelity, i.e. (finite) values of time at which the fidelity goes back to 1.

### III. FREE IDEAL EVOLUTION FOR A TRIPOD SYSTEM

#### A. Preliminaries

We consider the system introduced in [7] for holonomic quantum computation: see Fig. 1, where three degenerate levels are connected with a fourth one by Rabi oscillations. The adiabatic evolution of this system was analyzed in several papers for different experimental implementations [7, 9, 10, 31]. Here we review the ideal noiseless case, taking into account also non-adiabatic effects that are important in the presence of decoherence, when the loop cannot be completed in an arbitrarily long time. At time  $t = 0$  the logical states  $|0\rangle$  and  $|1\rangle$ , while  $|a\rangle$  is an ancilla state used as “buffer” during the evolution. The Hamiltonian

of the system reads

$$H(t) = |e\rangle\langle\Omega_0(t)\langle 0| + \Omega_1(t)\langle 1| + \Omega_a(t)\langle a| + \text{H.c.} \quad (3.1)$$

where  $\Omega_j(t)$  represent the time dependent Rabi frequencies of the transitions. The loop in the parameter space is obtained by varying  $\Omega_j(t)$  ( $j = 0, 1, a$ ). In our calculations we consider  $\Omega_j(t) \in \mathbb{R}, \forall t$ . The eigenvalues of the system are

$$\{0, \pm\sqrt{\Omega_0(t)^2 + \Omega_1(t)^2 + \Omega_a(t)^2} = \pm\Omega\}, \quad (3.2)$$

where 0 is 2-fold degenerate, corresponding to a 2-dimensional (computational) eigenspace, and  $\Omega$  is kept constant. Therefore, the parameter space is the 2-sphere

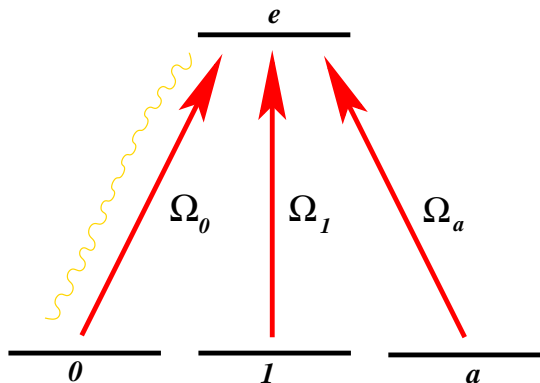


FIG. 1: (Color online) Scheme of a tripod system: 0 and 1 are computational levels, while  $a$  is an ancilla state used for the intermediate steps of the transformation. The three degenerate levels are connected with an upper level  $e$  by time dependent Rabi frequencies  $\Omega_j(t)$ . We also show the noise introduced in our analysis, that induces additional transitions between 0 and  $e$ .

of radius  $\Omega$ , given by  $\{\Omega_j \in \mathbb{R} | \sum_j \Omega_j^2 = \Omega^2\}$ . Introducing the parametrization

$$\Omega_1 = \Omega \sin \vartheta \cos \varphi, \quad \Omega_0 = \Omega \sin \vartheta \sin \varphi, \quad \Omega_a = \Omega \cos \vartheta, \quad (3.3)$$

the eigenstates take the form

$$\begin{aligned} |D_0(t)\rangle &= \cos \varphi |0\rangle - \sin \varphi |1\rangle, \\ |D_1(t)\rangle &= \cos \vartheta \sin \varphi |0\rangle + \cos \vartheta \cos \varphi |1\rangle - \sin \vartheta |a\rangle, \\ |D_{\pm}(t)\rangle &= (\pm |e\rangle + \sin \vartheta \sin \varphi |0\rangle + \sin \vartheta \cos \varphi |1\rangle + \cos \vartheta |a\rangle) / (\sqrt{2}). \end{aligned} \quad (3.4)$$

The computational space (belonging to the degenerate eigenvalue 0) is

$$C_S = \text{Span}\{|D_0(t)\rangle, |D_1(t)\rangle\}, \quad (3.5)$$

while  $|D_{\pm}(t)\rangle$  are the bright eigenstates belonging to  $\pm\Omega$ .

Applying the definition given in Section II, the elements of the adiabatic connection (2.10) for the

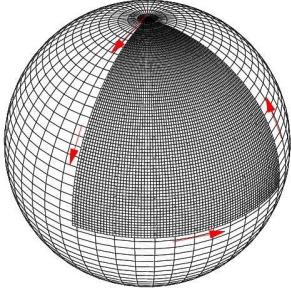


FIG. 2: (Color online) Path in parameter space for the realization of a NOT gate. The solid angle spanned during the evolution is  $\pi/2$ .

eigenspace  $m = 0$  are

$$A_\vartheta = 0, \quad A_\varphi = i\sigma_y \cos \vartheta, \quad (3.6)$$

where  $\sigma_y = -i(|D_0(t_0)\rangle\langle D_1(t_0)| - |D_1(t_0)\rangle\langle D_0(t_0)|)$ . The holonomy (2.9) for a closed loop on a sphere for the computational space reads

$$U_{\text{ad}} = \mathbf{P} e^{-\oint_C A_\varphi d\varphi} = e^{-i\sigma_y \oint_C \cos \vartheta d\varphi} = \exp(i\sigma_y \omega), \quad (3.7)$$

where  $\omega$  is the solid angle enclosed by the loop in the parameter space. As an explicit example (that will be considered in the following), let  $\omega = \pi/2$ , and obtain

$$U_{\pi/2} = \exp(i\sigma_y \pi/2) = i\sigma_y = \begin{pmatrix} 0 & 1 \\ -1 & 0 \end{pmatrix} \quad (3.8)$$

(in the basis  $\{|D_0(t_0)\rangle, |D_1(t_0)\rangle\}$ ), that represents a NOT transformation (up to a phase for the state  $|D_0\rangle$ ).

Following the discussion in the previous Section we discuss the non-adiabatic corrections to this system. In order to use Eq. (2.11), we will consider the loop shown in Fig. 2, obtained by going from the pole to the equator, spanning then a  $\pi/2$  angle and finally going back to the pole. The solid angle enclosed in this loop is equal to  $\pi/2$ ; in the adiabatic limit (when the product  $\Omega\tau$  goes to infinity,  $\tau$  being the total time of the cyclic evolution and  $\Omega$  the energy of the bright states) this path yields a NOT gate as in Eq. (3.8).

The first step consists in constructing the operator  $D$  from Eq. (3.4) and the definition (2.5); its matrix representation, written in the basis  $\{|D_i(t_0)\rangle\}_{i=0,1,+,-}$ , is

$$D(t, t_0) = -i \begin{pmatrix} 0 & \dot{\varphi} \cos \vartheta & \dot{\varphi} \sin \vartheta / \sqrt{2} & \dot{\varphi} \sin \vartheta / \sqrt{2} \\ -\dot{\varphi} \cos \vartheta & 0 & \dot{\vartheta} / \sqrt{2} & \dot{\vartheta} / \sqrt{2} \\ -\dot{\varphi} \sin \vartheta / \sqrt{2} & -\dot{\vartheta} / \sqrt{2} & 0 & 0 \\ -\dot{\varphi} \sin \vartheta / \sqrt{2} & -\dot{\vartheta} / \sqrt{2} & 0 & 0 \end{pmatrix}. \quad (3.9)$$

## B. Analytical results

One can see from Eq. (3.9) that, as far as the rate of change of the angles  $\varphi$  and  $\vartheta$  is constant in each segment of the path, we can use Eq. (2.11) to calculate the evolution operator along the path shown in Fig. 2. The complete expression is explicitly given in Appendix A.

A noteworthy feature of the exact expression is that it is factorized in three terms. In the adiabatic limit it simplifies to

$$U_{\pi/2}(\Omega\tau) = U_3(\Omega\tau_3) U_2(\Omega\tau_2) U_1(\Omega\tau_1) \xrightarrow{\tau\Omega \rightarrow \dagger\infty}$$

$$U_{\pi/2}^{\text{ad}}(\Omega\tau) = \begin{pmatrix} 0 & 1 & 0 & 0 \\ -1 & 0 & 0 & 0 \\ 0 & 0 & e^{-i\tau\Omega} & 0 \\ 0 & 0 & 0 & e^{+i\tau\Omega} \end{pmatrix}, \quad (3.10)$$

$\tau$  being the total evolution time needed for covering the loop in the parameter space and  $\tau_i = \alpha_i\tau$ , with  $\sum_i \alpha_i = 1$ . This represents a NOT gate for the de-

generate subspace and yields (fast oscillating) dynamical phases for the bright states.

## C. Fidelity revivals

In order to understand how far the evolution operator is from the ideal one, we use the fidelity, defined as

$$\begin{aligned} F(\tau) &= \text{Tr}\{\sigma_{\text{ad}}(\tau)\sigma(\tau)\} \\ &= \text{Tr}\{U_{\pi/2}^{\text{ad}}\sigma(0)U_{\pi/2}^{\text{ad}\dagger}U_{\pi/2}(\Omega\tau)\sigma(0)U_{\pi/2}^\dagger(\Omega\tau)\}, \end{aligned} \quad (3.11)$$

where  $\sigma(0)$  is the density operator describing the initial state, assumed to be pure, and  $\sigma_{\text{ad}}$  the corresponding operator for the adiabatic ideal evolution. The mean fidelity (averaged over a set of input states uniformly distributed on the Bloch sphere) is plotted in Fig. 3 as a function of the adiabaticity parameter  $\Omega\tau$ .

$F(\tau)$  asymptotically approaches the value 1 (with some oscillations), as expected (adiabatic limit). Interestingly,

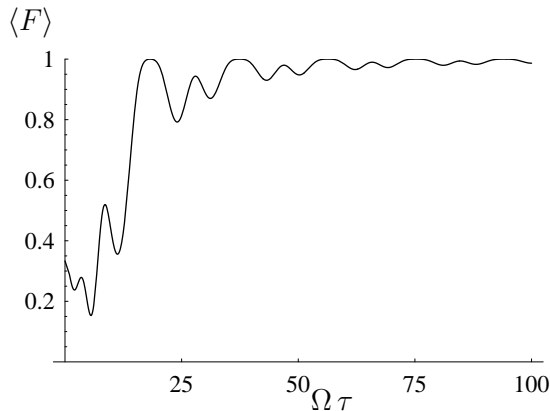


FIG. 3: Mean fidelity versus the cyclic time  $\Omega\tau$  (noiseless case).  $\Omega$  is the energy gap between the bright and dark states.  $\tau$  is the time needed to cover the loop shown in Fig. 2. The average is performed over a set of initial states uniformly distributed on the Bloch sphere.

the fidelity is exactly one for some *finite* values of time,  $\tau = \tau_k^*$ , that are clearly independent of the initial state. In this case the NOT transformation is perfect, even though one is far from the adiabatic regime. We now discuss this curious feature that will turn out to be of interest in the search for an optimal operation time at which the computation is most robust against noise (see Section V).

In order to obtain a formula for the times  $\tau_k^*$ , consider the operator

$$Q(\Omega\tau) = U_{\pi/2}^\dagger(\Omega\tau)U_{\pi/2}^{\text{ad}}(\Omega\tau) \quad (3.12)$$

appearing in Eq. (3.11). When the three arcs in the loop in Fig. 2 are covered in equal times, one obtains a lengthy analytical expression for  $Q$ , not reproduced here. In particular, the (1,1) element reads

$$Q_{11}(\Omega\tau) = \frac{4\Omega^2\tau^2 + 9\pi^2 \cos\left(\frac{\Omega\tau}{3}\sqrt{1 + \left(\frac{3\pi}{2\Omega\tau}\right)^2}\right)}{9\pi^2 + 4\Omega^2\tau^2} \quad (3.13)$$

and by equating the above expression to 1 one gets

$$\tau_k^* = \frac{3\pi}{2\Omega}\sqrt{16k^2 - 1}, \quad k \in \mathbb{N}^*. \quad (3.14)$$

In turn, this yields, by direct substitution in Eq. (3.12),

$$Q(\Omega\tau_k^*) = \begin{pmatrix} 1 & 0 & 0 & 0 \\ 0 & 1 & 0 & 0 \\ 0 & 0 & e^{-i\Omega\tau_k^*} & 0 \\ 0 & 0 & 0 & e^{+i\Omega\tau_k^*} \end{pmatrix}. \quad (3.15)$$

The first fidelity revival is obtained for  $k = 1$  and their approximate frequency reads

$$f(\tau, \Omega) = \frac{\Omega}{3}\sqrt{1 + \left(\frac{3\pi}{2\Omega\tau}\right)^2}. \quad (3.16)$$

From this equation it is clear that the periodicity of the maxima in Fig. 3 is only apparent (the frequency depends on  $\Omega\tau$ ). On the other hand, the second term in the square root is very small, even for the first peak, making  $f/\Omega$  approximately constant. The additional seemingly optimal points appearing in Fig. 3 (at approximately double frequency) are not solution of Eq. (3.14).

These revivals can be important for experimental applications: in principle they would enable one to obtain a perfect NOT transformation, without reaching the adiabatic regime. It is important to notice that this result does not depend on the initial state of the system but it is a feature of the chosen path: indeed the operator  $Q(\Omega\tau)$  does not contain any information about the initial state.

Finally, we emphasize that similar features (and in particular the presence of the revivals in the non-adiabatic regime) hold for a large class of gates. For transformations consisting in a loop which starts at the pole, spans a segment on a geodesics (the equator) and goes back to the pole enclosing a solid angle  $\omega = \pi/2n$  ( $n \in \mathbb{N}^*$ ) there is a straightforward generalization of Eq. (3.14):

$$\tau_k^*(n) = \frac{(2n+1)\pi}{2n\Omega}\sqrt{16k^2n^2 - 1}. \quad (3.17)$$

This expression is valid provided that the loop is covered at a constant angular speed:

$$\dot{\vartheta}_{\text{segment1}} = \dot{\varphi}_{\text{segment2}} = \dot{\vartheta}_{\text{segment3}} = \text{const.} \quad (3.18)$$

Reversing the orientation of the loops leads to identical results. These general observations can be of interest for experimental applications.

#### IV. NOISE AND MASTER EQUATION

A physical system is never completely isolated from its environment and, in order to take into account the effects produced by the latter, one analyzes the dynamics in terms of a master equation. In the usual approach to this problem one assumes that the Hamiltonian of the system is time independent (see for instance [32]). For time dependent Hamiltonians a slightly different approach is needed. Rigorous mathematical results were derived by Davies and Spohn [33]. We summarize here the main conclusions, providing for completeness a physical derivation in Appendix B, where emphasis is put on the physical meaning of the analysis in the context of adiabaticity and holonomic quantum computation.

We consider a general Liouville operator with a time dependent system Liouvillian

$$\mathcal{L}(t) = \mathcal{L}_0(t) + \mathcal{L}_{SB} = \mathcal{L}_S(t) \otimes 1 + 1 \otimes \mathcal{L}_B + \mathcal{L}_{SB}. \quad (4.1)$$

The evolution of density operator  $\rho(t)$ , describing the system and the environment, is governed by the von Neumann-Liouville equation

$$\dot{\rho}(t) = \mathcal{L}(t)\rho(t). \quad (4.2)$$

We assume that there are no initial correlations between system (whose density matrix is  $\sigma$ ) and bath (whose density matrix is  $\sigma_B$ ) and that the latter is in equilibrium (e.g. in a thermal state)

$$\varrho(0) = \sigma(0) \otimes \sigma_B, \quad \mathcal{L}_B \sigma_B = 0. \quad (4.3)$$

The key hypothesis in the derivation of a master equation is that the typical timescale of the evolution is much slower than the timescales characterizing the bath. The additional hypothesis in our case is that the timescale related to the rate of change of the system Hamiltonian is the slowest timescale of our problem, due to the adiabaticity of the evolution. In other words, compared to the bath correlation time, the evolution of  $\mathcal{L}_S$  is always ‘‘adiabatic.’’ This is assured by the condition

$$\tau_c \Delta \ll 1, \quad (4.4)$$

where  $\tau_c$  is the correlation time of the bath and the energy gap,  $\Delta = \min |\epsilon_n(t) - \epsilon_m(t)|$ , characterizes the rate of change of  $\mathcal{L}_S$ . Under these conditions one gets (Appendix B)

$$\dot{\sigma}(t) = [\mathcal{L}_S(t) + \Gamma(t)]\sigma(t), \quad (4.5)$$

where  $\sigma(t) = \text{Tr}_B \{\varrho(t)\}$  is the system density matrix and

$$\begin{aligned} \Gamma(t) &= \sum_{\omega} Q_{\omega}(t) \int_{-\infty}^0 du \text{Tr}_B \{ \mathcal{L}_{SB} \exp[-\mathcal{L}_0(t) u] \\ &\quad \times \mathcal{L}_{SB} \exp[\mathcal{L}_0(t) u] \sigma_B \} Q_{\omega}(t), \end{aligned} \quad (4.6)$$

$Q_{\omega}(t)$  being the instantaneous eigenprojections of  $\mathcal{L}_S$ ,

$$\begin{aligned} \mathcal{L}_S(t) &= i \sum_{\omega} \omega(t) Q_{\omega}(t), \\ \sum_{\omega} Q_{\omega}(t) &= 1, \quad Q_{\omega}(t) Q_{\omega'}(t) = \delta_{\omega\omega'} Q_{\omega}(t). \end{aligned} \quad (4.7)$$

Equation (4.5) is the same master equation one would obtain by considering  $\mathcal{L}_S(t)$  ‘‘frozen’’ at time  $t$  and evaluating the decay rates and the frequency shifts at the instantaneous eigenfrequencies  $\omega(t) = \epsilon_m(t) - \epsilon_n(t)$  of the system Liouvillian.

We now turn our attention to the physical system described in Sec. III. In terms of the total Hamiltonian,

$$\mathcal{L}(t)\rho = -i[H_T(t), \rho]. \quad (4.8)$$

For simplicity we consider an environment affecting only the transitions between levels  $|0\rangle$  and  $|e\rangle$ ; this is enough for our purposes. The total Hamiltonian is

$$H_T(t) = H(t) + H_B + \lambda H_{SB}, \quad (4.9)$$

where  $\lambda$  is a dimensionless scaling factor introduced for later convenience and representing the strength of the

noise, and  $H(t)$  is the system Hamiltonian (3.1). The bath is an ensemble of quantum harmonic oscillators,

$$H_B = \sum_k \omega_k a_k^{\dagger} a_k, \quad (4.10)$$

with  $\omega_k$  the frequency of the  $k$ -th mode. The interaction Hamiltonian is

$$H_{SB} = \sum_k \gamma_k (|0\rangle\langle e| + |e\rangle\langle 0|) \otimes (a_k^{\dagger} + a_k), \quad (4.11)$$

where  $\gamma_k$  is the coupling constant between the system and the  $k$ -th mode of the bath. By using Eq. (3.4) we can write

$$\begin{aligned} |e\rangle\langle 0| &= \frac{\cos \varphi}{\sqrt{2}} (|D_+(t)\rangle - |D_-(t)\rangle) \langle D_0(t)| \\ &+ \frac{\sin \varphi \cos \vartheta}{\sqrt{2}} (|D_+(t)\rangle - |D_-(t)\rangle) \langle D_1(t)| \\ &+ \frac{\sin \varphi \sin \vartheta}{2} (|D_+(t)\rangle - |D_-(t)\rangle) (\langle D_+(t)| + \langle D_-(t)|). \end{aligned} \quad (4.12)$$

In the interaction picture generated by the operator  $R$  defined in (2.4), the density operator reads

$$\rho_R(t) = R^{\dagger} \sigma(t) R. \quad (4.13)$$

By taking the time derivative of Eq. (4.13) we obtain

$$\dot{\sigma}(t) = R \dot{\rho}_R(t) R^{\dagger} + R [iD(t, 0), \rho_R(t)] R^{\dagger}. \quad (4.14)$$

By plugging Eqs. (4.12) and (4.14) in Eqs. (4.5) and (4.6), recalling the action (2.4) of  $R(t, 0)$  and considering that the eigenvalues of the Hamiltonian are time independent (Lamb shifts and decay rates will be time independent too), we obtain the following master equation:

$$\dot{\rho}_R(t) = -i[H_S(0), \rho_R(t)] - i[D(t, 0), \rho_R(t)] + \lambda^2 \Gamma[\rho_R(t)] \quad (4.15)$$

where

$$\begin{aligned} \Gamma[\rho_R(t)] &= \sum_{\alpha, \beta=0,1,\pm} f_{\alpha\beta}(t) \left( i\Delta_{\alpha\beta} [L_{\alpha\beta} L_{\alpha\beta}^{\dagger}, \rho_R(t)] \right. \\ &\quad \left. - \frac{\Gamma_{\alpha\beta}}{2} \left( \{L_{\alpha\beta} L_{\alpha\beta}^{\dagger}, \rho_R(t)\} - 2L_{\alpha\beta}^{\dagger} \rho_R(t) L_{\alpha\beta} \right) \right). \end{aligned} \quad (4.16)$$

The Lindblad operators read

$$L_{\alpha\beta} = |D_{\alpha}(0)\rangle\langle D_{\beta}(0)|, \quad (4.17)$$

while  $f_{\alpha\beta} = f_{\beta\alpha}$ , with

$$f_{\alpha 0} = \frac{\cos^2 \varphi}{2}, \quad f_{\alpha 1} = \frac{\sin^2 \varphi \cos^2 \vartheta}{2}, \quad f_{\alpha \pm} = \frac{\sin^2 \varphi \sin^2 \vartheta}{4} \quad (4.18)$$

and  $f_{00} = f_{11} = f_{01} = 0$ .

In the case of a thermal bath the Lamb shifts and the decay rates read

$$\begin{aligned}\Delta_{\alpha\beta} &= P \int_{-\infty}^{\infty} d\omega \frac{\xi_{\text{th}}(\omega)}{\omega - \epsilon_{\alpha} + \epsilon_{\beta}}, \\ \Gamma_{\alpha\beta} &= 2\pi \xi_{\text{th}}(\epsilon_{\alpha} - \epsilon_{\beta})\end{aligned}\quad (4.19)$$

where  $P$  denotes the principal value,

$$\begin{aligned}\xi_{\text{th}}(\omega) &= \xi(\omega)[n_B(\omega) + 1] + \xi(-\omega)n_B(-\omega) \\ &= \frac{1}{2}\xi(\omega) \left[ \coth \frac{\beta\omega}{2} + 1 \right] \\ &\quad + \frac{1}{2}\xi(-\omega) \left[ \coth \frac{\beta\omega}{2} - 1 \right]\end{aligned}\quad (4.20)$$

is the thermal spectral density,  $\xi(\omega)$  being the bare spectral density of the noise [ $\xi(\omega) = 0$  for  $\omega < 0$ ]

$$\xi(\omega) = \sum_k \gamma_k^2 \delta(\omega_k - \omega)\quad (4.21)$$

and  $n_B(\omega) = 1/(\exp(\beta\omega) - 1)$  the mean number of bosons at frequency  $\omega$ .

Notice that a non vanishing temperature entails an effective modification of the form factors of the interaction, making them in general unbounded from below [34]. Moreover, note that when  $\epsilon_{\alpha} = \epsilon_{\beta}$ , Eqs. (4.19) particularize to

$$\Delta_{\alpha\alpha} = \int_0^{\infty} d\omega \frac{\xi(\omega)}{\omega}, \quad \Gamma_{\alpha\alpha} = 2\pi \frac{\xi'(0^+)}{\beta}\quad (4.22)$$

and the Lamb shift  $\Delta_{\alpha\alpha}$  is temperature independent.

## V. EVOLUTION IN PRESENCE OF NOISE: OPTIMAL WORKING POINT

Equation (4.15) was numerically integrated along the loop in Fig. 2 when the three arcs are covered at a constant angular speed. We set  $\Gamma_{+0} = \Gamma_{+1} = \Gamma_{0-} = \Gamma_{1-} = 1.1\Omega$ ,  $\Gamma_{0+} = \Gamma_{-0} = \Gamma_{1+} = \Gamma_{-1} = 0.8\Omega$ ,  $\Gamma_{++} = \Gamma_{--} = 1\Omega$ ,  $\Gamma_{+-} = 1.2\Omega$ ,  $\Gamma_{-+} = 0.7\Omega$ ,  $\Delta_{+0} = \Delta_{+1} = \Delta_{0-} = \Delta_{1-} = -1.1\Omega$ ,  $\Delta_{0+} = \Delta_{-0} = \Delta_{1+} = \Delta_{-1} = 0.8\Omega$ ,  $\Delta_{++} = \Delta_{--} = 1\Omega$ ,  $\Delta_{+-} = -1.2\Omega$ , and  $\Delta_{-+} = 0.7\Omega$ . These values of the Lamb shifts and decay rates are physically meaningful and have been chosen, somewhat arbitrarily, for illustrative purposes. We will consider later the realistic case of an Ohmic bath at different temperatures and will directly derive the values of all the constants from Eq. (4.19).

In Fig. 4 we show the behavior of the fidelity for three different initial states. In each graph, from top to bottom, the dissipation constant increases from  $\lambda^2 = 0$  to 0.05.

In the noiseless case (upper line in the three plots) the fidelity tends to 1 when  $\Omega\tau \rightarrow \infty$  (adiabatic limit). This asymptotic value is not reached monotonically: there are some oscillations, with maxima at  $F = 1$  in the noiseless

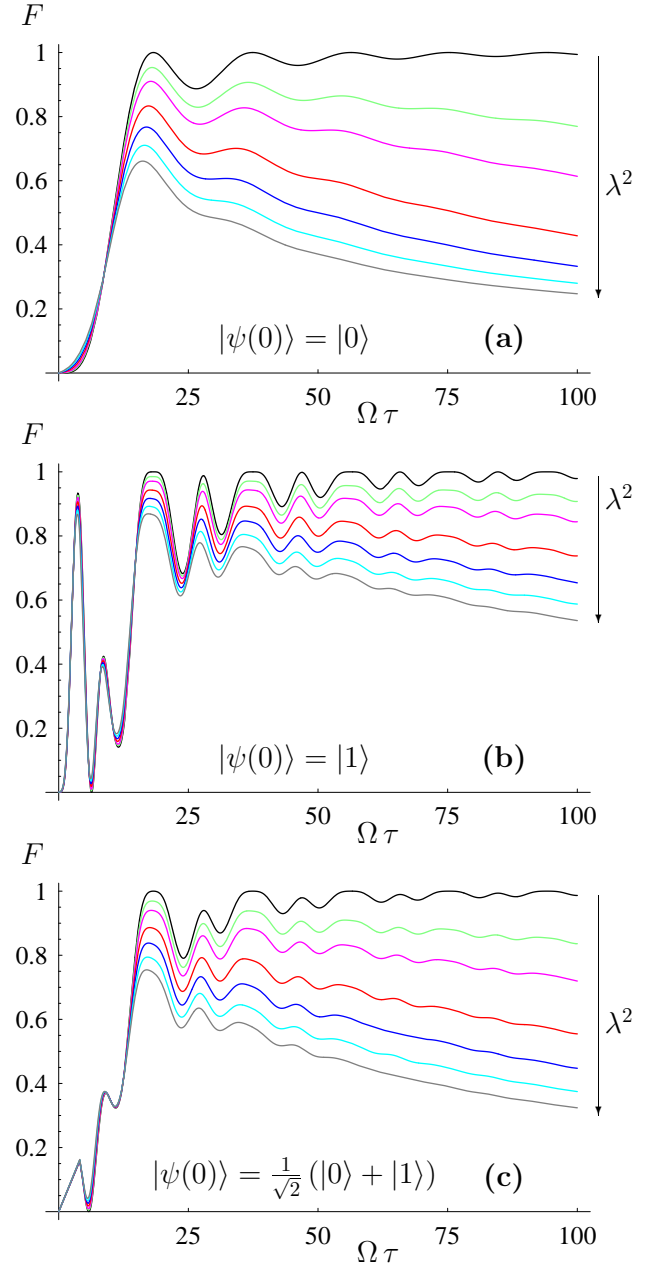


FIG. 4: (Color online) Fidelity  $F$  versus cyclic time  $\Omega\tau$  for three different initial states,  $\Omega$  being the energy gap between the bright and dark states and  $\tau$  the time needed to cover the loop shown in Fig. 2 (NOT gate). (a) “up” state; (b) “down” state; (c) completely symmetric state. In each graph the dissipation constant  $\lambda^2$ , defined in Eq. (4.15), increases from top to bottom:  $\lambda^2 = 0$  (noiseless case), 0.005, 0.01, 0.02, 0.03, 0.04 and 0.05.

case. This is the case discussed in Section III: the NOT transformation is perfect, even though one is far from the adiabatic regime, at the time values given by (3.14).

Notice that although the oscillations and the general behavior of  $F$  depend on the initial state, the overall trend is of general validity and only depends on the path



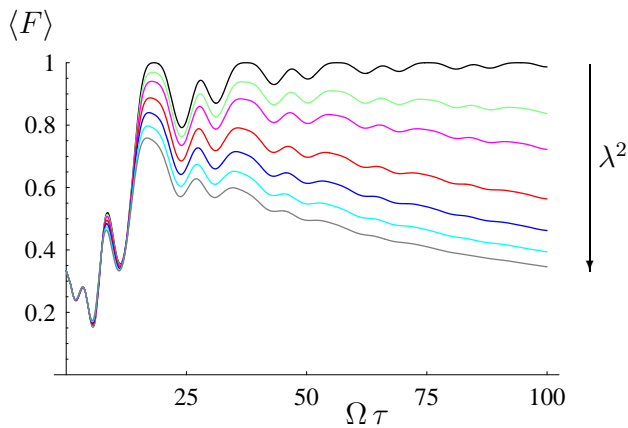


FIG. 5: (Color online) Mean fidelity  $\langle F \rangle$  versus cyclic time  $\Omega\tau$ . All parameters are identical to those of Fig. 4.

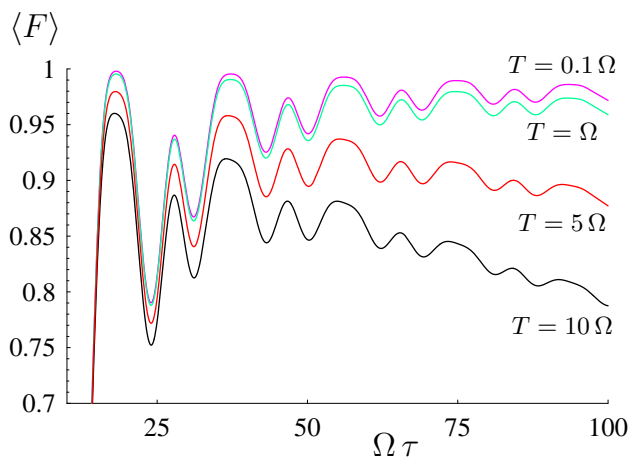


FIG. 6: (Color online) Mean fidelity  $\langle F \rangle$  versus cyclic time  $\Omega\tau$ , evaluated for an Ohmic spectral density at different temperatures  $T = \beta^{-1}$ , with  $\lambda^2 = 0.01$ . Notice the different scale on the vertical axis, as compared to the previous figures.

in the parameter space and the speed at which it is covered. Interestingly, the position of these maxima is only weakly dependent on noise: the horizontal shifts of the peaks are almost irrelevant. (This is due to the small influence of the Lamb shifts.) The mean fidelity (averaged over a set of input states uniformly distributed over the Bloch sphere) is displayed in Fig. 5. One observes all the interesting features discussed before.

For all the above reasons, we can estimate the value of the optimal gate-operation point for experimental applications as that point corresponding to the first peak. An important remark is however in order: in the non adiabatic regime, the gate is no longer purely geometrical. Both dynamical and geometrical effects contribute to the transformation and cannot be easily separated, because in general the generators do not commute. In principle it would be possible to extract the geometrical contribution, but one would not gain any additional information, useful for experimental purposes.

In general, in the presence of noise, the fidelity decreases as the time needed for the transformation increases. This can make it difficult to obtain a pure geometrical transformation (because of the necessary adiabatic condition). This problem could be slightly reduced by choosing a large energy gap between the degenerate computational space and the bright states. However, it seems more convenient to exploit the presence of the peaks and partially neglect this physical request. As a matter of fact, the fidelity decrease due to the noise is very small in the non adiabatic regime. This makes the NOT gate feasible by using a fine tuning of the total operation time. The best performance is obtained for an *optimal operation time*

$$\tau^* = \tau_{k=1}^* = \frac{3\pi}{2\Omega} \sqrt{15} \quad (5.1)$$

corresponding to the first peak of the fidelity.

On the other hand, some interesting features of the fidelity do depend on the initial states and are apparent in Fig. 4. Some states are less robust than others; this is due to the fact that, during the evolution, the population transfer between the levels depends on the initial state: thus, the longer the population “lives” in a level which is subject to noise, the less efficient is the transformation. A critical point is obviously the total amount of noise. In our simulations we have considered a noise strength  $\lambda^2$  ranging from 0.5% to 5%. A realistic physical estimate yields a noise not exceeding 0.5%. In this regime the fidelity at the optimal point reaches values greater than 0.9 for all the states considered. From this result it is clear that we can exploit the optimal times for realizing the NOT transformation with a relatively high fidelity even in absence of additional control.

These general conclusions can be corroborated by considering a particular spectral density for the environment: Figure 6 display the behavior of the mean fidelity for an Ohmic spectral density

$$\xi(\omega) = \kappa \omega \exp(-\omega/\omega_c) \quad (5.2)$$

at different temperatures. We used Eq. (4.19) and set  $\kappa = 1/100$ ,  $\omega_c = 100\Omega$  and  $T = 1/\beta = \Omega/10, \Omega, 5\Omega, 10\Omega$ , corresponding to a thermal bath at low, intermediate, high and very high temperatures, respectively. Notice that the mean fidelity is always higher than 80% in the whole range of times considered (up to  $100\Omega\tau$ ). In particular, at the optimal time, fidelity decreases only up to a few percent, even in the very high temperature case.

As already emphasized at the end of Sec. III, these results can be extended to more general loops, yielding optimal times like in Eq. (3.17). This can be of interest for experimental applications.

## VI. CONCLUSIONS

We studied some aspects of holonomic quantum computation by focusing our attention on a particular physical system, shown in Fig. 1, undergoing a loop in the



parameter space that, in the adiabatic limit, yields a NOT gate. We derived a general expression for the evolution operator, without taking the adiabatic limit. After specializing this formula to a specific loop, an exact expression for the propagator was obtained. In order to gain more physical insight we considered the fidelity of the transformation compared to the adiabatic one. We found that there exist some values for the duration of the evolution for which the fidelity is equal to 1, even though one is far from the adiabatic regime. The presence of these peaks is important for experimental applications: if the total operation time can be fine tuned to the first peak, one can realize a transformation which is the most robust against noise. In particular, we considered several initial conditions and analyzed the effects of quantum noise on the evolution of the system (if the rate of change of the system Hamiltonian is much smaller than the typical timescales of the thermal bath). As an example, we considered a particular noise, inducing transition outside the computational space, and obtained the relevant master equation. Its numerical solution yielded information on the behavior of the fidelity and showed how important the optimal points is: actually, it enables one to obtain (without external additional control) high values of the fidelity before the system suffers much from the detrimental consequences of the noise. It will be important to understand whether and how this feature can be of help when one tries to control the system in order to reduce decoherence and dissipation.

We conclude by emphasizing that the strategy sug-

gested in this article in order to minimize the effects of decoherence, being based on the determination of a (finite, non adiabatic) optimized operation time, is somewhat different from the other strategies suggested so far for suppressing decoherence. Clearly, these observations can be of interest for experimental applications. One should try and understand whether the fidelity revivals, and consequently optimal operation times, exist also for two-qubit gates.

### Acknowledgments

This work was supported by the European Community through contracts EuroSQIP, IST-SQUBIT2, IST-TOPQIP. One of us (G.F.) thanks Scuola Normale Superiore in Pisa for their kind hospitality and support.

### APPENDIX A

We give here the exact analytical expressions of the operators that describe the evolution of the system in the loop shown in Fig. 2. A straightforward but lengthy calculation yields (in the basis  $\{|D_i(0)\}_{i=0,1,+,-}$ )

$$U_{\pi/2}(\Omega\tau) = U_3(\Omega\tau_3) U_2(\Omega\tau_2) U_1(\Omega\tau_1) \quad (\text{A1})$$

with (we set  $\tau_1 = \tau_2 = \tau_3 = \tau/3$  for simplicity)

$$U_1(\Omega\tau/3) = \begin{pmatrix} 1 & 0 & 0 & 0 \\ 0 & \frac{\pi \sin \alpha}{2\alpha} & \cos \alpha - \frac{i\Omega\tau \sin \alpha}{3\sqrt{2}\alpha} & \frac{3\alpha \cos \alpha + i\Omega\tau \sin \alpha}{3\sqrt{2}\alpha} \\ 0 & -\frac{\sqrt{2}(2i\Omega\tau + 3\pi \cos \alpha)}{\beta} & \frac{3\pi + 2i\Omega\tau \cos \alpha + 6\alpha \sin \alpha}{\beta} & \frac{-3\pi - 2i\Omega\tau \cos \alpha + 6\alpha \sin \alpha}{\beta} \\ 0 & \frac{\sqrt{2}(2i\Omega\tau - 3\pi \cos \alpha)}{\beta^*} & \frac{-3\pi + 2i\Omega\tau \cos \alpha + 6\alpha \sin \alpha}{\beta^*} & \frac{3\pi - 2i\Omega\tau \cos \alpha + 6\alpha \sin \alpha}{\beta^*} \end{pmatrix}, \quad (\text{A2})$$

$$U_2(\Omega\tau/3) = \begin{pmatrix} \frac{\pi \sin \alpha}{2\alpha} & \cos \alpha & \frac{-i\Omega\tau \sin \alpha}{3\sqrt{2}\alpha} & \frac{i\Omega\tau \sin \alpha}{3\sqrt{2}\alpha} \\ \frac{-(4\Omega^2\tau^2 + 9\pi^2 \cos \alpha)}{36\alpha^2} & \frac{\pi \sin \alpha}{2\alpha} & \frac{i\pi\Omega\tau(-1 + \cos \alpha)}{6\sqrt{2}\alpha^2} & \frac{-i\pi\Omega\tau(-1 + \cos \alpha)}{6\sqrt{2}\alpha^2} \\ \frac{i\pi\Omega\tau(-1 + \cos \alpha)}{6\sqrt{2}\alpha^2} & \frac{-i\Omega\tau \sin \alpha}{3\sqrt{2}\alpha} & \frac{9\pi^2 + 2\Omega^2\tau^2 + 2\Omega^2\tau^2 \cos \alpha}{36\alpha^2} & \frac{-\Omega^2\tau^2(-1 + \cos \alpha)}{18\alpha^2} \\ \frac{-i\pi\Omega\tau(-1 + \cos \alpha)}{6\sqrt{2}\alpha^2} & \frac{i\Omega\tau \sin \alpha}{3\sqrt{2}\alpha} & \frac{-\Omega^2\tau^2(-1 + \cos \alpha)}{18\alpha^2} & \frac{9\pi^2 + 2\Omega^2\tau^2 + 2\Omega^2\tau^2 \cos \alpha}{36\alpha^2} \end{pmatrix}, \quad (\text{A3})$$

$$U_3(\Omega\tau/3) = \begin{pmatrix} \frac{\pi \sin \alpha}{2\alpha} & 0 & -\frac{\sqrt{2}(2i\Omega\tau+3\pi \cos \alpha)}{\beta} & \frac{\sqrt{2}(2i\Omega\tau-3\pi \cos \alpha)}{\beta^*} \\ 0 & 1 & 0 & 0 \\ \frac{3\alpha \cos \alpha - i\Omega\tau \sin \alpha}{3\sqrt{2}\alpha} & 0 & \frac{3\pi+2i\Omega\tau \cos \alpha+6\alpha \sin \alpha}{\beta} & \frac{-3\pi+2i\Omega\tau \cos \alpha+6\alpha \sin \alpha}{\beta^*} \\ \frac{3\alpha \cos \alpha + i\Omega\tau \sin \alpha}{3\sqrt{2}\alpha} & 0 & \frac{-3\pi-2i\Omega\tau \cos \alpha+6\alpha \sin \alpha}{\beta} & \frac{3\pi-2i\Omega\tau \cos \alpha+6\alpha \sin \alpha}{\beta^*} \end{pmatrix}, \quad (\text{A4})$$

where  $\alpha = \sqrt{9\pi^2 + 4\Omega^2\tau^2}/6$  and  $\beta = 6\pi + 4i\Omega\tau$ . These are the operators appearing in Eq. (3.10) [with  $\tau_i = \tau/3$ ,  $i = 1, 2, 3$  and the angular velocities in Eq. (3.11) kept constant].

## APPENDIX B

We derive here the master equation (4.5), by focusing on the physical aspects of the proof, in the context of quantum computation with holonomic gates.

Let us start by considering the Liouville operator (4.1) acting on density matrices  $\rho$ . Consider a density operator  $\varrho(t)$  describing the system and the environment. Its evolution is governed by the von Neumann-Liouville equation (4.2), with the initial condition (4.3). In the interaction picture engendered by the free Liouvillian  $\mathcal{L}_0(t)$ ,

$$\Phi_0(t, 0) = \mathbf{T} \exp \left\{ \int_0^t \mathcal{L}_0(s) ds \right\}, \quad (\text{B1})$$

the density matrix takes the form

$$\varrho_I(t) = \Phi_0^{-1}(t, 0) \varrho(t) \quad (\text{B2})$$

and Eq. (4.2) reads

$$\dot{\varrho}_I(t) = \mathcal{L}_{SB}(t, 0) \varrho_I(t), \quad (\text{B3})$$

where

$$\mathcal{L}_{SB}(t, 0) = \Phi_0^{-1}(t, 0) \mathcal{L}_{SB} \Phi_0(t, 0). \quad (\text{B4})$$

By formally integrating (B3) we get

$$\varrho_I(t) = \mathbf{T} \exp \left\{ \int_0^t \mathcal{L}_{SB}(s, 0) ds \right\} \varrho(0), \quad (\text{B5})$$

whose expansion up to second order in the interaction Liouvillian  $\mathcal{L}_{SB}$  reads

$$\begin{aligned} \varrho_I(t) = & \left[ 1 + \int_0^t ds \mathcal{L}_{SB}(s, 0) \right. \\ & \left. + \int_0^t ds \int_0^s du \mathcal{L}_{SB}(s, 0) \mathcal{L}_{SB}(u, 0) \right] \varrho(0). \end{aligned} \quad (\text{B6})$$

The reduced density operator of the system is obtained by tracing (B6) over the bath:

$$\begin{aligned} \sigma_I(t) &= \text{Tr}_B \{ \varrho_I(t) \} \\ &= \sigma(0) + \int_0^t ds \text{Tr}_B \{ \mathcal{L}_{SB}(s, 0) \varrho(0) \} \\ &\quad + \int_0^t ds \int_0^s du \text{Tr}_B \{ \mathcal{L}_{SB}(s, 0) \mathcal{L}_{SB}(u, 0) \varrho(0) \}. \end{aligned} \quad (\text{B7})$$

The second term in this expansion vanishes for a bath at equilibrium (4.3). Therefore Eq. (B7) can be written as

$$\begin{aligned} \sigma_I(t) &= \sigma(0) + \\ &\quad + \int_0^t ds \Phi_S^{-1}(s, 0) \left[ \int_0^s du K(s, u) \right] \Phi_S(s, 0) \sigma(0), \end{aligned} \quad (\text{B8})$$

where

$$\Phi_S(t, 0) = \mathbf{T} \exp \left\{ \int_0^t \mathcal{L}_S(s) ds \right\}, \quad (\text{B9})$$

$$K(s, u) = \text{Tr}_B \left\{ \mathcal{L}_{SB} \tilde{\mathcal{L}}_{SB}(s, u) \sigma_B \right\} \quad (\text{B10})$$

and

$$\tilde{\mathcal{L}}_{SB}(s, u) = \Phi_0(s, u) \mathcal{L}_{SB} \Phi_0^{-1}(s, u). \quad (\text{B11})$$

At this point one assumes that the typical timescale of the evolution is much slower than the timescales characterizing the bath and derives a master equation in the Markov approximation. We make a further hypothesis, justified by the physical nature of the process we intend to study. In our system (2.2)-(2.3) there is another timescale, related to the rate of change of the system Hamiltonian: we assume that this is the slowest timescale of our problem, due to the adiabaticity of the evolution and then, compared to the bath correlation time, the evolution of  $\mathcal{L}_S$  is always ‘‘adiabatic.’’ This is assured by the condition (4.4). This condition allows us to write

$$\begin{aligned} \Phi_S(s, u) &= \mathbf{T} \exp \left\{ \int_u^s \mathcal{L}_S(t) dt \right\} \\ &\simeq \mathbf{T} \exp \left\{ \int_u^s \mathcal{L}_S(s) dt \right\} = \exp \{ \mathcal{L}_S(s)(s - u) \} \end{aligned} \quad (\text{B12})$$

when  $|s-u| < \tau_c$ . Moreover the bath correlation function rapidly vanishes for times larger than the correlation time  $\tau_c$

$$K(s, u) \simeq 0, \quad \text{for } |s-u| > \tau_c. \quad (\text{B13})$$

Using Eqs. (B10) and (B12) we obtain

$$K(s, u) \simeq \text{Tr}_B \left\{ \mathcal{L}_{SB} \exp[\mathcal{L}_0(s)(s-u)] \right. \\ \left. \times \mathcal{L}_{SB} \exp[-\mathcal{L}_0(s)(s-u)] \sigma_B \right\} \quad (\text{B14})$$

and thus, in the secular approximation, forced by Davies's projection,  $\sum_\omega Q_\omega(s)[\dots]Q_\omega(s)$ ,

$$\Gamma(s) = \sum_\omega Q_\omega(s) \left[ \int_0^s du K(s, u) \right] Q_\omega(s) \\ \simeq \sum_\omega Q_\omega(s) \int_{-\infty}^0 du \text{Tr}_B \left\{ \mathcal{L}_{SB} \exp[-\mathcal{L}_0(s)u] \right. \\ \left. \times \mathcal{L}_{SB} \exp[\mathcal{L}_0(s)u] \sigma_B \right\} Q_\omega(s), \quad (\text{B15})$$

where  $Q_\omega(s)$ , given by (4.7), are the instantaneous eigenprojections of  $\mathcal{L}_S$ . Therefore, Eq. (B8) takes the form

$$\sigma_I(t) = \sigma(0) + \int_0^t ds \Phi_S^{-1}(s, 0) \Gamma(s) \Phi_S(s, 0) \sigma(0), \quad (\text{B16})$$

which yields the differential equation

$$\dot{\sigma}_I(t) = \Phi_S^{-1}(t, 0) \Gamma(t) \Phi_S(t, 0) \sigma_I(t). \quad (\text{B17})$$

Going back to the Schrödinger picture,

$$\dot{\sigma}(t) = \Phi_S(t, 0) \sigma_I(t), \quad (\text{B18})$$

we finally get

$$\dot{\sigma}(t) = [\mathcal{L}_S(t) + \Gamma(t)] \sigma(t). \quad (\text{B19})$$

This is the master equation (4.5): it is the same equation one would obtain by considering  $\mathcal{L}_S(t)$  "frozen" at time  $t$ , by applying the standard Markov approximation and evaluating the decay rates and the frequency shifts at the instantaneous eigenfrequencies  $\omega(t) = \epsilon_m(t) - \epsilon_n(t)$  of the system Liouvillian. This supports our physical intuition of a system Hamiltonian adiabatically changing in a faster environment.

- 
- [1] M.A. Nielsen and I.L. Chuang, *Quantum Computation and Quantum Information* (Cambridge University Press, Cambridge, 2000).
- [2] G. Benenti, G. Casati and G. Strini, *Principles of Quantum Computation and Information* (World Scientific, Singapore, 2004).
- [3] *Geometric phases in physics*, A. Shapere and F. Wilczek Eds., (World Scientific, Singapore, 1989).
- [4] A. Bohm, A. Mostafazadeh, H. Koizumi, Q. Niu and J. Zwanziger, *The Geometric Phase in Quantum Systems*, (Springer, 2003).
- [5] J. Jones *et al*, Nature, **403**, 869 (2000); A. Ekert *et al*, J. Mod. Opt. **47** 2501 (2000).
- [6] P. Zanardi and M. Rasetti, Phys. Lett. A **264**, 94 (1999). J. Pachos and P. Zanardi, Int. J. Mod. Phys. B **15**, 1257 (2001).
- [7] L. M. Duan, J. I. Cirac and P. Zoller, Science **292**, 1695 (2001).
- [8] G. Falci *et al*, Nature **407**, 355 (2000).
- [9] L. Faoro, J. Siewert and R. Fazio, Phys. Rev. Lett. **90**, 028301 (2003).
- [10] P. Solinas *et al*, Phys. Rev. A **67**, 062315 (2003).
- [11] D. Giulini, E. Joos, C. Kiefer, J. Kupsch, I.-O. Stamatescu, and H.-D. Zeh, *Decoherence and the Appearance of a Classical World in Quantum Theory* (Springer, Berlin, 1996).
- [12] D. Ellinas, S.M. Barnett, and M.A. Dupertuis, Phys. Rev. A **39**, 3228 (1989).
- [13] D. Gamliel and J.H. Freed, Phys. Rev. A **39**, 3238 (1989).
- [14] G. De Chiara and G.M. Palma Phys. Rev. Lett. **91**, 090404 (2003).
- [15] R.S. Whitney and Y. Gefen, Phys. Rev. Lett. **90**, 190402 (2002).
- [16] R.S. Whitney *et al.*, Phys. Rev. Lett. **94**, 070407 (2005).
- [17] A. Carollo *et al.*, Phys. Rev. Lett. **90**, 160402 (2003).
- [18] M.S. Sarandy and D.A. Lidar, Phys. Rev. A **71**, 012331 (2005).
- [19] M. Ericsson *et al.*, Phys. Rev. A **67**, 020101(R) (2003).
- [20] K.-P. Marzlin, S. Ghose, and B.C. Sanders, Phys. Rev. Lett **93**, 260402 (2004).
- [21] I. Kamleitner, J.D. Cresser, and B.C. Sanders, Phys. Rev. A **70**, 044103 (2004).
- [22] P. Solinas, P. Zanardi, and N. Zanghì Phys. Rev. A **70**, 042316 (2004).
- [23] D. Parodi, M. Sassetti, P. Solinas, P. Zanardi and N. Zanghì, quant-ph/0510056.
- [24] I. Fuentes-Guridi, F. Girelli, and E.R. Livine, Phys. Rev. Lett. **94**, 020503 (2005).
- [25] M.S. Sarandy and D.A. Lidar, quant-ph/0507012.
- [26] J. Anandan, Phys. Lett. A **133**, 171 (1988).
- [27] Y. Aharonov and J. Anandan, Phys. Rev. Lett. **58**, 1593 (1987).
- [28] A. Blais and A.-M. S. Tremblay, Phys. Rev. A **67**, 012308 (2003).
- [29] M. V. Berry, Proc. Roy. Soc. London, Ser. A **392**, 45 (1984).
- [30] F. Wilczek and A. Zee, Phys. Rev. Lett. **52**, 2111 (1984); A. Zee, Phys. Rev. A **38**, 1 (1988).
- [31] R. Unanyan, M. Fleischhauer, B.W. Shore and K. Bergmann Opt. Comm. **155**, 144 (1998); R. G. Unanyan, B.W. Shore and K. Bergmann Phys. Rev. A, **59**, 2910 (1999).

- [32] C. W. Gardiner, P. Zoller, *Quantum Noise*, 2nd Ed., (Springer, Berlin, 2000).
- [33] E. B. Davies and H. Spohn, *J. Stat. Phys.* **19**, 511 (1978).
- [34] P. Facchi, S. Tasaki, S. Pascazio, H. Nakazato, A. Tokuse and D. A. Lidar, *Phys. Rev. A* **71**, 022302 (2005).